Elastic Metamaterials with Simultaneously Negative Effective Shear Modulus and Mass Density

Ying Wu,[1,2] Yun Lai,[1,3] and Zhao-Qing Zhang[1,*]

[1]*Department of Physics, Hong Kong University of Science and Technology, Clear Water Bay, Kowloon, Hong Kong, China*
[2]*Division of Mathematical and Computer Sciences and Engineering, King Abdullah University of Science and Technology, Thuwal 23955-6900, Saudi Arabia*
[3]*Department of Physics, Soochow University, 1 Shizi Street, Suzhou 215006, People's Republic of China*

(Received 22 February 2011; revised manuscript received 11 July 2011; published 2 September 2011)

We propose a type of elastic metamaterial comprising fluid-solid composite inclusions which can possess a negative shear modulus and negative mass density over a large frequency region. Such a material has the unique property that only transverse waves can propagate with a negative dispersion while longitudinal waves are forbidden. This leads to many interesting phenomena such as negative refraction, which is demonstrated by using a wedge sample and a significant amount of mode conversion from transverse waves to longitudinal waves that cannot occur on the interface of two natural solids.

DOI: 10.1103/PhysRevLett.107.105506 PACS numbers: 81.05.Xj, 42.25.Gy, 46.40.−f, 62.30.+d

Recently, the artificial electromagnetic (EM) materials denoted as metamaterials have attracted a great deal of attention due to their unusual properties. One example is the left-handed material (LHM), which was first predicted by Veselago [1]. LHM is a material with simultaneously negative permittivity and permeability, which leads to EM waves propagating with the wave vector opposite to the Poynting vector. LHM gives rise to many intriguing phenomena, such as negative refraction, a reversed Doppler shift [1], a perfect lens [2], etc. The first realization of LHM for EM waves consisting of metallic wires and split rings was proposed by Pendry *et al.* [3] and fabricated by Smith *et al.* [4]. Thereafter, enormous progress has been made in realizing negative refraction with metamaterials in various frequency regimes [5–8].

Very recently, the principle of metamaterial has been extended to acoustic and elastic media, and various schemes have been proposed to realize acoustic and elastic LHM [9–15]. A normal elastic medium can propagate both longitudinal and transverse waves, which is different from EM and acoustic media. In an isotropic solid, these waves are described by three independent material parameters, i.e., mass density ρ, bulk modulus κ, and shear modulus μ. Analogous to EM metamaertials, negative effective elastic parameters can be realized by introducing resonant structures into the building blocks of an elastic metamaterial. For example, due to dipolar resonances in locally resonant rubber-coated-lead structures [9,16] and thin membranes [10,17,18], these structures have been shown to achieve negative mass density. Air bubbles in water [9,11] and the Helmholtz resonator [12,19] can achieve a negative bulk modulus as a result of monopolar resonances. It has also been found that the negative shear modulus is related to quadrupolar resonance [20,21]. However, to the best of our knowledge, there has been no report of resonant structures to realize the negative shear modulus with a noticeable bandwidth.

Finding the negative effective shear modulus is not only of scientific interest, but also has intriguing applications. For instance, if an elastic LHM has simultaneously negative density and a shear modulus in a certain frequency regime, it may give rise to the negative phase velocity of transverse waves, i.e., $c_t = \sqrt{\mu}\sqrt{1/\rho} < 0$, which implies negative refraction. Meanwhile, if the material's bulk modulus is positive and the longitudinal wave becomes evanescent, the elastic LHM can be used as a polarizer. It will be shown later that the total mode conversion from shear waves to longitudinal waves (and vice versa) can also be achieved when such a metamaterial is put in contact with a normal solid. This is not possible for any two natural solids. Here, we propose a new type of elastic metamaterial with a fluid-solid composite. Such a composite can support both dipolar and quadrupolar resonances in its building blocks and produce a simultaneously negative effective mass density and negative effective shear modulus in a large frequency region, resulting in a wide negative band for shear waves and a gap for longitudinal waves. The effective medium parameters for ρ, κ, and μ can be obtained from an effective medium theory (EMT) [20]. The existence of a large negative band is confirmed by the band structure calculations using the multiple-scattering theory (MST) [22]. The negative refraction is demonstrated by MST simulations with a wedge sample. Interestingly, we find a significant amount of mode conversion from shear waves to longitudinal waves induced by the double-negative property of the metamaterial. Such a large conversion only happens under negative refraction and, therefore, does not occur in any natural solids.

The two-dimensional elastic metamaterial proposed in this work is composed of cylindrical fluid-solid composite inclusions arranged in a triangular lattice in the x-y plane embedded in a host of polyethylene foam (HD115). The purpose of using a triangular lattice is to ensure isotropic dispersions near the Γ point of the metamaterial [23]. The

microstructure of the building block is shown in Fig. 1(a). The cylindrical inclusion is a water cylinder of radius $r_w = 0.24a$ coated by a layer of silicone rubber of outer radius $r_s = 0.32a$, where a is the lattice constant. In addition to quadrupolar resonance, the presence of a soft silicone rubber layer also introduces dipolar resonance which gives rise to negative mass density [16]. The water cylinder is chosen to enhance the quadupolar resonance as water can be easily deformed due to its zero shear modulus. The slippery boundary condition has been used on the interface between water and rubber. Compared to the air that was used in previous works [20,21], the larger mass density of water helps to provide the necessary momentum that is needed in any resonance. The material parameters are $\rho_w = 1.0 \times 10^3$ kg/m^3, $\lambda_w = 2.22 \times 10^9$ N/m^2, and $\mu_w = 0$ for water; $\rho_r = 1.3 \times 10^3$ kg/m^3, $\lambda_r = 6.0 \times 10^5$ N/m^2, and $\mu_r = 4.0 \times 10^4$ N/m^2 for silicone rubber [16]; and $\rho_f = 115$ kg/m^3, $\lambda_f = 6.0 \times 10^6$ N/m^2, and $\mu_f = 3.0 \times 10^6$ N/m^2 for foam [21]. Here λ is the Lamé constant, which is related to the bulk modulus through the relation $\kappa = \lambda + \mu$ in two dimensions. The velocities of longitudinal and transverse waves are defined by $c_l = \sqrt{\kappa + \mu}\sqrt{1/\rho}$ and $c_t = \sqrt{\mu}\sqrt{1/\rho}$, respectively. It can be seen that the wave speeds inside the silicone rubber are much smaller than those in the foam matrix and the water core. These large mismatches at the two interfaces enhance the dipolar and quadrupolar resonances and give rise to a broad negative band for shear waves.

The effective medium parameters of the above metamaterial, i.e., effective mass density, ρ_e, bulk modulus, κ_e, and shear modulus, μ_e, can be calculated by using the EMT developed by us, i.e., Eq. (3) in Ref. [20]. The results are plotted in Fig. 1(b), in which the black solid, red dashed, and blue short-dashed curves represent ρ_e, κ_e, and μ_e, respectively. Also plotted in Fig. 1(b) is the sum of the effective shear modulus and bulk modulus, i.e., $\kappa_e + \mu_e$, which is shown by the green dashed-dotted curve. The frequency is shown in the dimensionless unit $\tilde{f} = fa/c_{t0}$, where c_{t0} is the transverse wave speed in the matrix foam. Figure 1(b) clearly shows that ρ_e is negative in a large frequency region from $\tilde{f} = 0.149$ to $\tilde{f} = 0.263$. Within this regime, μ_e is also negative in a large frequency region from $\tilde{f} = 0.167$ [denoted by A in Fig. 1(b)] to $\tilde{f} = 0.216$ [denoted by B in Fig. 1(b)]. This overlap of negative ρ_e and negative μ_e regimes indicates that the effective refractive index for transverse waves should also be negative within the frequency region from A to B. It should be noted that $\kappa_e + \mu_e$ also has a small negative value in the regime from $\tilde{f} = 0.208$ to $\tilde{f} = 0.213$, which implies a negative band for longitudinal waves in this small frequency region.

To verify the prediction of the EMT, we have calculated the band structure by using the MST [22]. The full band structure is plotted in Fig. 2(a), from which we can see that the dispersion relation is isotropic and negative near the Γ point. Along the ΓM direction there exists a wide negative band (for shear waves) from $\tilde{f} = 0.161$ to $\tilde{f} = 0.218$ (denoted by red dots) as well as a narrow negative band (for longitudinal waves) from $\tilde{f} = 0.213$ to $\tilde{f} = 0.218$ (denoted by blue dots). The above results are consistent with the effective medium prediction shown in Fig. 1(b). In Fig. 2(b), we plot the transmission spectra for longitudinal and transverse waves passing through a slab sample of thickness $6a$ and width $50a$ by solid (blue) and dashed (red) curves, respectively. The incident wave is generated by passing a plane wave through a slit of width $20a$, and is incident normally onto the sample surface whose normal is along the ΓM direction. The transmission was obtained by integrating the flux along the incident direction at the output surface and dividing it by the integrated flux in the absence of the slab. Figure 2(b) shows clearly a passing band (transmission close to unity) for pure shear

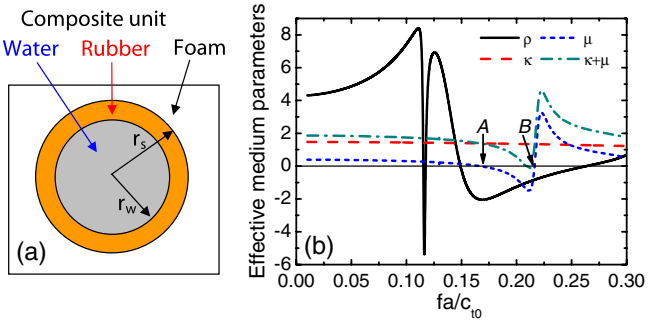

FIG. 1 (color online). (a) A schematic figure of the building block of the metamaterial: a rubber-coated water cylinder embedded in a foam host. (b) Effective medium parameters obtained from EMT. Solid (black), dashed (red), short-dashed (blue), and dash-dotted (cyan) curves correspond to effective medium parameters, ρ_e, κ_e, μ_e, and $\kappa_e + \mu_e$, respectively.

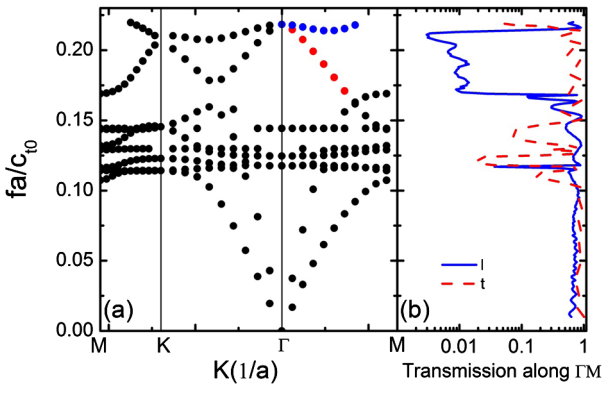

FIG. 2 (color online). (a) Band structure of a triangular array of rubber-coated water cylinders embedded in foam host as shown in Fig. 1(b). (b) The solid curve (blue) is the transmission coefficient for the longitudinal wave incidence and the dashed curve (red) is for the transverse wave incidence along the ΓM direction.

waves from $\tilde{f} = 0.170$ to $\tilde{f} = 0.213$, while a band gap is shown for longitudinal waves. The oscillations inside the band are due to Fabry-Perot resonances. These results agree well with the band structures shown in Fig. 2(a).

A negative effective refractive index leads to negative refraction. In order to demonstrate this interesting phenomenon, we use a wedge sample of the metamaterial, which is shown schematically in Fig. 3(a). The wedge sample has 90° and 60° corners, and the two perpendicular surfaces of the wedge are chosen to have their normals along the ΓM (horizontal) and ΓK (vertical) directions of the lattice, respectively. A plane transverse wave passing through a slit of width $20a$ is incident normally on the vertical surface of the wedge along the ΓM direction. It is clearly seen that the wave penetrates through the wedge and is refracted by the oblique surface. In Fig. 3(a), we can see that if the angle θ is positive under a positive incident angle i, then negative refraction occurs. To avoid the reflected waves coming from the bottom surface of the wedge due to internal reflections, we added a little absorption to the last few layers at the bottom of the wedge. In the simulation, we choose $\tilde{f} = 0.2$ as our working frequency and calculate both the near-field and far-field energy flux distributions, i.e., the time averaged Poynting vector, $j_k = \pi f \mathrm{Im}(\sigma_{ik} u_i^*)$, where u_i and σ_{ik} are, respectively, the displacement vector and stress tensor obtained from the MST [24]. The equifrequency contour [13] is plotted in the left panel of Fig. 3(b), in which the dashed ΓK line represents the surface normal of the oblique surface of the wedge. The other dashed line parallel to the ΓK line provides the conservation of the component of the wave vector parallel to the exit surface. This is shown in the right panel of Fig. 3(b), where the red dashed and blue short-dashed circles represent, respectively, the transverse and longitudinal modes inside the foam host, and the green solid circle corresponds to the eigenmodes inside the metamaterial. Thick blue and thin black arrows indicate, respectively, the directions of group velocities and phase velocities. Figure 3(b) clearly demonstrates that an oblique transverse wave incidence on the edge of the metamaterial wedge would result in negative refractions of both longitudinal and transverse waves in the background. The results of the energy flux calculations are shown in Figs. 3(c) and 3(d) for the near field and far field, respectively. Both results show unambiguously negative refraction. Because of the vector nature of elastic wave, the refracted waves in the far field can be separated into transverse and longitudinal components, which are represented by the dashed (red) and solid (black) curves in Fig. 3(d), respectively. It can be seen that the flux distributions reach their peaks at $\theta = 33°$ for transverse waves and at $\theta = 52°$ for longitudinal waves, respectively, which are consistent with Fig. 3(b). The near field shown in Fig. 3(c), however, cannot be separated easily due to the interference of the longitudinal and transverse waves.

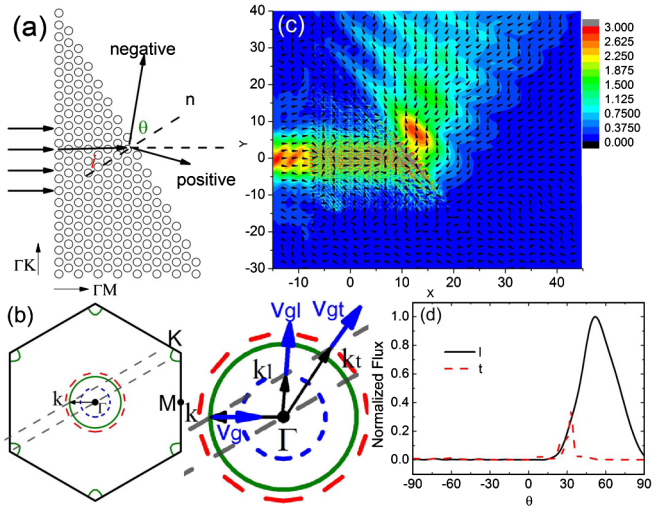

FIG. 3 (color online). (a) Schematic figure of the sample. i and θ are incident and refracted angles, respectively. n is the surface normal of the interface between the metamaterial and the host. ΓM and ΓK directions are along horizontal and vertical directions, respectively. The incident wave is coming from the left, shooting normally onto the vertical surface of the wedge. (b) (Left) The equifrequency surface in the $\boldsymbol{k}$ space of the foam (red dashed curve for transverse modes and blue short-dashed curve for longitudinal modes) and the metamaterial (green solid curve) at $\tilde{f} = 0.2$. Brillouin zone is depicted by solid back lines. (Right) The enlarged inner part of the equifrequency surface. $\mathbf{v}_g$ and $\boldsymbol{k}$ are the group velocity and wave vector inside the metamaterial, respectively. $\mathbf{k}_l$ ($\mathbf{v}_{gl}$) and $\mathbf{k}_t$ ($\mathbf{v}_{gt}$) are longitudinal and transverse wave vectors (group velocities) inside the host, respectively. (c) Total flux distribution for a transverse wave incidence on the wedge. The colors and arrows represent the magnitude and directions, respectively. (d) The far-field total flux distribution for the transverse wave incidence. Solid (black) and dashed (red) curves correspond to longitudinal and transverse waves, respectively.

More interesting, we note that the far-field flux distribution (as can been seen from the full width at half maximum of the peak) of the longitudinal wave is much larger than that of the transverse wave. This indicates a significant amount of mode conversion from transverse to longitudinal waves has occurred on the output surface of the wedge due to negative refraction. We have integrated the two distributions from $\theta = -90°$ to 90° and find that the ratio of the total outgoing far-field flux of the longitudinal wave to that of the transverse waves is around 11. Such an efficient mode conversion is a unique property of the double-negative elastic metamaterial. In fact, total mode conversion between shear waves and longitudinal waves can occur on an interface between a double-negative elastic metamaterial and a normal elastic medium under certain conditions. For example, consider a transverse plane wave in a double-negative elastic metamaterial of $\rho_1 < 0$ and $\mu_1 < 0$ is incident on the interface with a normal elastic medium ($\rho_2 > 0$, $\mu_2 > 0$, and $\kappa_2 > 0$), as shown

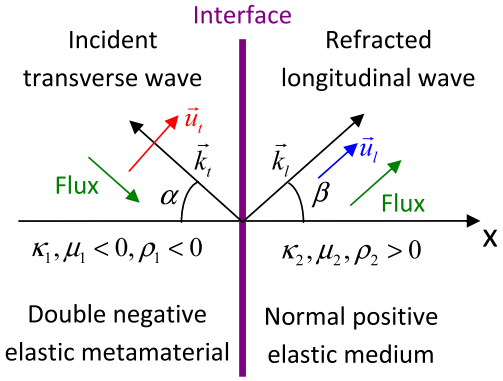

FIG. 4 (color online). A schematic graph of s-p mode conversion on the interface between a double-negative elastic metamaterial and a normal elastic medium.

in Fig. 4, and the refracted wave is longitudinal wave. The displacements in two media are $\vec{u}_t = u_t(\sin\alpha\hat{x} + \cos\alpha\hat{y})\, e^{ik_t(-\cos\alpha x + \sin\alpha y)}$ for the transverse wave and $\vec{u}_l = u_l(\cos\beta\hat{x} + \sin\beta\hat{y}) e^{ik_l(\cos\beta x + \sin\beta y)}$ for the longitudinal wave, where α and β are, respectively, the incidence and negative refraction angles. The continuity of displacement on the interface, i.e., $x = 0$, requires that $u_l = u_t$ and $\alpha + \beta = \pi/2$. This implies that only in the case of negative refraction can the mode conversion from transverse waves to longitudinal waves be complete, i.e., 100%, because the displacements of transverse waves ($\vec{u}_t$) and longitudinal waves ($\vec{u}_l$) can only be matched on the interface when the refraction angle is negative. With some simple derivation [25] we find the total mode conversion (and no reflection) conditions are given by Eq. (S3) in Ref. [25], i.e., $-\mu_1 = \mu_2 \tan 2\alpha \tan\alpha$, $\kappa_2 = \mu_2/\cos 2\alpha$, and $\tan\alpha = \frac{k_l}{k_t} = \frac{\sqrt{\mu_1/\rho_1}}{\sqrt{(\kappa_2+\mu_2)/\rho_2}}$ and the negative refraction angle is $\beta = \pi/2 - \alpha$. The incidence and refraction angles have similar forms as the Brewster angle in the EM case [26], where the incident angle satisfies $\tan i_B = \frac{n'}{n} = \frac{k'}{k}$, with n and n' being the refractive indices of incidence and refraction, and the refraction angle is equal to $\pi/2 - i_B$. However, the occurrence of total mode conversion is more stringent and complex than the Brewster angle. In the Brewster angle case, only one reflected wave is disappearing and Brewster angle always exists on the interface between any two dielectric materials. In contrast, total mode conversion in the elastic wave case requires the simultaneous disappearance of three waves, i.e., two in the reflection geometry and one in the refraction geometry, and such a novel phenomenon can only be achieved by using negative fraction metamaterials with specific elastic parameters as the incidence angle should satisfy four equations, i.e., Eq. (S3), simultaneously. The total mode conversion from longitudinal waves to transverse waves can also be realized under certain conditions [25]. It is worth mentioning that although total mode conversion is not possible on the interface between two normal solids, it can occur in a normal solid with a free surface, but in reflected waves [27].

To conclude, we have proposed a type of elastic metamaterial consisting of a triangular lattice of rubber-coated water cylinders in a foam matrix. Both the EMT and the band structure calculation show the existence of a negative band for shear waves in a large frequency region induced by simultaneous negative mass density and a shear modulus, which are produced by the enhanced dipolar and quadrupolar resonances, respectively. The absence of the longitudinal band in the frequency region makes the metamaterial a good candidate for a polarization filter. Negative refraction has been demonstrated by a wedge sample. Accompanying negative refraction, we also observed a significant amount of mode conversion from transverse waves to longitudinal waves, which has proved to be a unique property of double-negative elastic metamaterials. This phenomenon is an analogue to its electromagnetic counterpart, i.e., total transmission in the Brewster angle case, however, in a much more complex manner.

The work is supported by Hong Kong RGC Grant No. 605008, and start-up packages from KAUST and Soochow University.

*phzzhang@ust.hk

[1] V. G. Veselago, Sov. Phys. Usp. **10**, 509 (1968).
[2] J. B. Pendry, Phys. Rev. Lett. **85**, 3966 (2000).
[3] J. B. Pendry *et al.*, Phys. Rev. Lett. **76**, 4773 (1996); J. B. Pendry *et al.*, IEEE Trans. Microwave Theory Tech. **47**, 2075 (1999).
[4] D. R. Smith *et al.*, Phys. Rev. Lett. **84**, 4184 (2000); R. A. Shelby, D. R. Smith, and S. Schultz, Science **292**, 77 (2001).
[5] C. M. Soukoulis, S. Linden, and M. Wegener, Science **315**, 47 (2007).
[6] H. J. Lezec, J. A. Dionne, and H. A. Atwater, Science **316**, 430 (2007).
[7] J. Valentine *et al.*, Nature (London) **455**, 376 (2008).
[8] J. Yao *et al.*, Science **321**, 930 (2008).
[9] Y. Q. Ding *et al.*, Phys. Rev. Lett. **99**, 093904 (2007).
[10] S. H. Lee *et al.*, Phys. Rev. Lett. **104**, 054301 (2010).
[11] J. Li and C. T. Chan, Phys. Rev. E **70**, 055602 (2004).
[12] S. Zhang, L. Yin, and N. Fang, Phys. Rev. Lett. **102**, 194301 (2009).
[13] L. Feng *et al.*, Phys. Rev. Lett. **96**, 014301 (2006).
[14] M. H. Lu, L. Feng, and Y. F. Chen, Mater. Today **12**, 34 (2009).
[15] G. W. Milton, New J. Phys. **9**, 359 (2007).
[16] Z. Liu *et al.*, Science **289**, 1734 (2000).
[17] Z. Yang *et al.*, Phys. Rev. Lett. **101**, 204301 (2008).
[18] S. H. Lee *et al.*, Phys. Lett. A **373**, 4464 (2009).
[19] N. Fang *et al.*, Nature Mater. **5**, 452 (2006).
[20] Y. Wu, Y. Lai, and Z. Q. Zhang, Phys. Rev. B **76**, 205313 (2007).
[21] X. Zhou and G. Hu, Phys. Rev. B **79**, 195109 (2009).

[22] I. E. Psarobas, N. Stefanou, and A. Modinos, Phys. Rev. B **62**, 278 (2000); Z. Liu *et al.*, *ibid.* **62**, 2446 (2000); J. Mei *et al.*, *ibid.* **67**, 245107 (2003); J. Mei *et al.*, Phys. Rev. Lett. **96**, 024301 (2006); Y. Lai and Z. Q. Zhang, Appl. Phys. Lett. **83**, 3900 (2003).
[23] Y. Wu and Z. Q. Zhang, Phys. Rev. B **79**, 195111 (2009).
[24] Y. Wu *et al.*, Phys. Rev. B **77**, 125125 (2008).
[25] See Supplemental Material at http://link.aps.org/supplemental/10.1103/PhysRevLett.107.105506 for a demonstration of total mode conversion.
[26] For example, J. D. Jackson, *Classical Electrodynamics* (John Wiley & Sons, Inc., New York, 1999), 3rd ed.
[27] For example, D. Royer and E. Dieulesaint, *Elastic Waves in Solids I* (Springer, New York, 1999).